

# EXTRINSIC MESHLESS COLLOCATION METHODS FOR PDES ON MANIFOLDS\*

MENG CHEN<sup>†</sup> AND LEEVAN LING<sup>‡</sup>

**Abstract.** We proposed ways to implement meshless collocation methods extrinsically for solving elliptic partial differential equations on smooth, closed, connected and complete Riemannian manifolds with arbitrary codimensions. Our methods are based on strong-form collocations with oversampling and least-squares minimizations, which can be implemented either analytically or approximately. By restricting global kernels to the manifold, our methods resemble their easy-to-implement domain-type analogies, i.e., Kansa methods. Our main theoretical contribution is the robust convergence analysis under some standard smoothness assumptions for high order convergence. Numerical demonstrations are provided to verify the proven convergence rates and we simulate reaction-diffusion equations for generating Turing patterns on manifolds.

**Key words.** Kernel-based methods, Kansa methods, Radial basis functions, Convergence analysis.

**AMS subject classifications.** 65D15, 65N35, 41A63.

**1. Introduction.** Throughout this paper, we use  $d_{\mathcal{M}}$  to denote dimension of some manifold  $\mathcal{M} \subset \mathbb{R}^d$ , whose codimension is given as  $r := d - d_{\mathcal{M}}$ . We consider a general second-order strongly elliptic equation on  $\mathcal{M}$  in the form of

$$\mathcal{L}_{\mathcal{M}}u := (-a\Delta_{\mathcal{M}} + \vec{b} \cdot \nabla_{\mathcal{M}} + c)u = f. \quad (1.1)$$

We assume coefficients  $a, \vec{b}, c \in \mathcal{W}_{\infty}^{m-2}(\mathcal{M})$ ,  $f \in L^2(\mathcal{M})$ , and the existence [54] of classical solutions  $u^*$  to (1.1) in Hilbert spaces  $\mathcal{H}^m(\mathcal{M})$ . The manifold gradient operator  $\nabla_{\mathcal{M}}$  and the Laplace-Beltrami operator  $\Delta_{\mathcal{M}}$  in (1.1) will be defined later in (3.2) and (3.3).

In recent years, many numerical methods have been developed for solving the surface problem by means of some intrinsic, extrinsic or embedding techniques. Intrinsic methods use local parametrization in  $d_{\mathcal{M}}$ -dimensional coordinates [5, 37]. Spatial discretization of extrinsic methods are imposed on surface nodes/meshes without leaving the surfaces [10, 21]. They may require analytical transformations of differential operators on the surface to standard ones in Cartesian (or extrinsic) coordinates or projections. Methods in the embedding class avoid such transformations by extending surface PDEs into some embedding spaces in  $\mathbb{R}^d$  and work with  $d$ -dimensional computational domains, see [4, 8, 18, 31, 32, 33, 34, 44, 46]. One potential disadvantage is the additional computational cost due to the extension, particularly for high codimensions.

A great deal of meshless radial basis functions (RBFs) approaches has been proposed initially for PDEs on spheres. The standard RBFs were applied to produce positive definite kernels for divergence-free fields of tangent vectors on spheres [12, 14, 39]. Some developed an interpolant approximation by using multiscale compactly supported RBFs restricted on spheres [26] and it was applied to meshless collocation technique for solving PDEs on spheres [27]. There are also some existing error estimates for RBF interpolations on spheres [52], as well as on manifolds generally

---

\*This work was supported by a Hong Kong Research Grant Council GRF Grant.

<sup>†</sup>Department of Mathematics, Nanchang University, Nanchang, China (chenmeng821@sina.com).

<sup>‡</sup>Department of Mathematics, Hong Kong Baptist University, Kowloon Tong, Hong Kong (lling@hkbu.edu.hk).

[13]. In [53], a novel discretization method of meshless collocation approximation was described for solving semilinear parabolic equations on Euclidean spheres. Recent papers were introduced by making use of localized kernel bases [11, 48]. Besides, the local meshless RBF approach [48] and a global one in [15] were respectively utilized to approximate surface differential operators without information about curvatures of manifolds.

Unsymmetric meshless strong-form collocation methods, also known as Kansa methods [23, 24], are simple to implement and have been widely used in many physics and engineering applications [7, 25, 28, 42]. It is known that the exactly determined formulation in the original Kansa method could lead to singular linear systems [22]. Solvability, stability and convergence can be recovered via some overdetermined formulations [9, 29, 30, 47].

Because of our interest in some computationally efficient meshless formulations, we aim to derive collocation methods for PDEs that are generally sufficient to work on any smooth, closed, connected and complete Riemannian manifolds with any codimension embedded in  $\mathbb{R}^d$  [40]. Given two discrete sets of points on  $\mathcal{M}$ , namely *collocation points* in  $X$  and *trial centers* in  $Z$ , we employ some kernels  $\Psi_m : \mathcal{M} \times \mathcal{M} \rightarrow \mathbb{R}$  with the smoothness order  $m$  that reproduce  $\mathcal{H}^m(\mathcal{M})$ . Spanned by such translation-invariant  $\Psi_m$ , some finite-dimensional *trial spaces*  $\mathcal{U}_Z$  can be defined by

$$\mathcal{U}_Z = \mathcal{U}_{Z, \mathcal{M}, \Psi_m} := \text{span}\{\Psi_m(\cdot - z^j) \mid z^j \in Z\}. \quad (1.2)$$

In this paper, we analyze the following *least-squares solution*

$$U_{X, Z} := \arg \inf_{u \in \mathcal{U}_Z} \sum_{x \in X} \|\mathcal{L}_{\mathcal{M}} u(x) - f(x)\|_2^2 \quad (1.3)$$

from  $\mathcal{U}_Z$  in (1.2). The following theorem gives an error estimate in terms of fill distances  $h_\bullet$  and mesh ratios  $\rho_\bullet$  of  $X$  and  $Z$ , whose formal definitions can be found in (3.5) and (3.6), for the proposed least-squares solution (1.3) under the assumptions in Sections 2 and 3.

**THEOREM 1.1.** *Let  $k \geq 2$ . Suppose that assumptions A1–A4 in Sections 2 and 3 hold for some integer  $m \geq \lceil k + 1 + d_{\mathcal{M}}/2 \rceil$  and let  $u^* \in \mathcal{H}^m(\mathcal{M})$  be the classical solution to (1.1). Then the least-squares solution  $U_{X, Z} \in \mathcal{U}_Z$  defined by (1.3) satisfies the estimate*

$$\|U_{X, Z} - u^*\|_{\mathcal{H}^k(\mathcal{M})} \leq C h_Z^{m-d_{\mathcal{M}}/2} \left( h_Z^{-k} + h_X^{-k+2} h_Z^{-2} \right) \|u^*\|_{\mathcal{H}^m(\mathcal{M})} \quad (1.4)$$

for some constant  $C$  depending only on  $k$ ,  $\mathcal{M}$ ,  $\mathcal{L}_{\mathcal{M}}$ ,  $\Psi_m$  and the mesh ratio  $\rho_X$  of  $X$ , as well as sufficiently small  $h_X < h_Z$  in the sense of (3.13).

In Section 2, some definitions and notations essential to Theorem 1.1 will be provided. Section 3 contains the proof of Theorem 1.1 after proving some necessary lemmas. In Section 4, we show how the least-squares solution (1.3) can be sought either by an analytical or by a kernel-based approximation approach. In Section 5, we present two numerical experiments to verify the proven convergent property and to compare the proposed methods with each other, as well as with other algorithms in the literatures. Finally, we verify robustness of the proposed methods by simulating Turing patterns on surfaces.

**2. Sobolev spaces on manifolds and embedding domains.** Firstly, we need all the assumptions on the manifold  $\mathcal{M}$  so that an inverse inequality for kernel-based

trial functions in [20] can be applied in Section 3.

A1. Let  $\mathcal{M}$  be a closed, connected and complete Riemannian manifold of  $\mathbb{R}^d$  such that it is of class  $\mathcal{C}^{m+1}$  for some integer  $m$ . We further suppose as required in [20] that  $\mathcal{M}$  satisfies

- (Bounded geometry). If the injectivity radius  $r_{\mathcal{M}}$  of  $\mathcal{M}$  is positive and covariant derivatives of the Riemannian metric are bounded, then  $\mathcal{M}$  is of bounded geometry.
- (Boundary regularity). If  $c_1 r_{\mathcal{M}}^{d_{\mathcal{M}}} \leq \text{vol}(\mathcal{B}(x, r)) \leq c_2 r_{\mathcal{M}}^{d_{\mathcal{M}}}$ ,  $0 < c_1 < c_2 < \infty$ , holds for any ball  $\mathcal{B}(x, r)$  with the radius  $0 \leq r \leq r_{\mathcal{M}}$ .

For such  $\mathcal{C}^{m+1}$  Riemannian manifolds, let  $\mathcal{T}_p \mathcal{M}$  denote the tangent space at each point  $p \in \mathcal{M}$ . Moreover, the  $r$ -dimensional normal space of  $\mathcal{M}$  at  $p$  is spanned by some orthonormal bases  $\{\vec{n}_i(p)\}_{i=1}^r$ . By these bases, we define the  $d \times r$  matrix of unit normal bases

$$N(p) := [\vec{n}_1(p), \dots, \vec{n}_r(p)]. \quad (2.1)$$

In this paper, we develop kernel-based methods that work solely on the manifold  $\mathcal{M}$ . Yet, our convergence analysis calls upon certain embedding techniques and theories. Formally, we suppose as in [33] that  $\mathcal{M}$  is smooth enough. By [33, Thm. 3.8], there exists some  $\delta_{\mathcal{M}} > 0$  such that the Euclidean *closest point restriction map*

$$R_{\text{cp}}(x) := \arg \inf_{p \in \mathcal{M}} \|p - x\|_2 \quad (2.2)$$

is well-defined and, for any  $\delta \in (0, \delta_{\mathcal{M}}]$ , is of class  $\mathcal{C}^m$  in the  $\delta$ -narrow band domain

$$\Omega_{\delta} := \{x \in \mathbb{R}^d : \|x - p\|_2 \leq \delta, \text{ for some } p \in \mathcal{M}\}. \quad (2.3)$$

We denote  $\Omega_{\mathcal{M}} := \Omega_{\delta_{\mathcal{M}}}$  to be the largest possible narrow band domain that allows  $\mathcal{C}^m$  restriction maps. If we operate on sets, then we have  $R_{\text{cp}}(\Omega_{\delta}) = \mathcal{M}$  for any  $\delta \in (0, \delta_{\mathcal{M}}]$ .

For any embedding domain  $\Omega \subset \mathbb{R}^d$ , we will work in standard Sobolev spaces  $\mathcal{W}_l^k(\Omega)$  with some  $k \in \mathbb{N}$ , see [1]. They consist of all functions  $u$  with distributional derivatives  $D_x^{\alpha} u$  in  $L^l(\Omega)$  for all  $|\alpha| \leq k$  and associate with norms

$$\|u\|_{\mathcal{W}_l^k(\Omega)} := \begin{cases} \left( \sum_{|\alpha| \leq k} \int_{\Omega} |D_x^{\alpha} u(x)|^l dx \right)^{1/l} & \text{for } 1 \leq l < \infty, \\ \max_{|\alpha| \leq k} \left( \text{ess sup}_{x \in \Omega} |D_x^{\alpha} u(x)| \right) & \text{for } l = \infty. \end{cases} \quad (2.4)$$

For Sobolev spaces  $\mathcal{W}_l^k(\mathcal{M})$  on manifolds, we adopt the definition in [54]. Functions in  $\mathcal{W}_l^k(\mathcal{M})$  are characterized by some  $\mathcal{C}^k$  atlas  $\{(V_i, \varphi_i)\}_{i \in \Lambda}$  and a subordinate partition of unity  $\{\varrho_i\}_{i \in \Lambda}$  in  $\mathcal{C}_0^k(\mathcal{M})$ . The corresponding norms are defined by

$$\|u\|_{\mathcal{W}_l^k(\mathcal{M})} := \begin{cases} \left( \sum_{|\beta| \leq k} \sum_{i \in \Lambda} \|D_{\theta}^{\beta} \{(\varrho_i u) \circ \varphi_i^{-1}(\theta)\}\|_{L^l(\varphi_i(V_i))}^l \right)^{1/l} & \text{for } 1 \leq l < \infty, \\ \max_{|\beta| \leq k} \sum_{i \in \Lambda} \|D_{\theta}^{\beta} \{(\varrho_i u) \circ \varphi_i^{-1}(\theta)\}\|_{L^{\infty}(\varphi_i(V_i))} & \text{for } l = \infty. \end{cases} \quad (2.5)$$

In the case of  $l = 2$ ,  $\mathcal{W}_2^k(\mathcal{M})$  coincides with the Hilbert space  $\mathcal{H}^k(\mathcal{M})$ . For any discrete set  $\Xi = \{p^1, \dots, p^{n_{\Xi}}\}$  of  $n_{\Xi}$  points on  $\mathcal{M}$ , discrete norms [19, Rem.17] on  $\Xi$

are defined as

$$\|u\|_{\ell_l(\Xi)} := \begin{cases} \left( \sum_{j=1}^{n_\Xi} |u(p^j)|^l \right)^{1/l} & \text{for } 1 \leq l < \infty, \\ \max_{1 \leq j \leq n_\Xi} |u(p^j)| & \text{for } l = \infty. \end{cases} \quad (2.6)$$

With these notations, we give a special case of norm equivalence between  $\mathcal{M}$  and  $\Omega_\delta$  as follows. As a direct consequence of chain rules and A1, this allows us to go between the distributional derivatives  $D_x^\alpha$  in (2.4) and  $D_\theta^\beta$  in (2.5) for the  $x$ - and  $\theta$ -space respectively.

LEMMA 2.1. *Suppose that the manifold  $\mathcal{M}$  satisfies the assumption A1. Let  $\Omega_\delta$  be defined as that in (2.3) with any sufficiently small  $\delta < \delta_{\mathcal{M}}$ . Then there exist some constants  $0 < C_1 \leq C_2$  depending only on  $\mathcal{M}$ ,  $d$  and  $k$  such that*

$$C_1 \delta^{(d-d_{\mathcal{M}})/2} \|u\|_{\mathcal{H}^k(\mathcal{M})} \leq \|u \circ R_{\text{cp}}\|_{\mathcal{H}^k(\Omega_\delta)} \leq C_2 \delta^{(d-d_{\mathcal{M}})/2} \|u\|_{\mathcal{H}^k(\mathcal{M})}$$

holds for any  $u \in \mathcal{H}^m(\mathcal{M})$  and  $0 \leq k \leq m$ .

PROOF. This lemma is a straightforward generalization of [8, Lem. 3.1] from  $r = d - d_{\mathcal{M}} = 1$  to arbitrary codimensions. To prove the lemma, we consider any nearby translated manifold  $\mathcal{M}_v = \{p + N(p)v \mid p \in \mathcal{M}\}$  for any  $v \in \mathbb{R}^r$  with  $\|v\|_{\ell_2(\mathbb{R}^d)} < \delta_{\mathcal{M}}$ . Then,  $N(p)v$  is normal to  $\mathcal{M}$  and we have  $\|u \circ R_{\text{cp}}\|_{\mathcal{H}^k(\mathcal{M}_v)} = \|u\|_{\mathcal{H}^k(\mathcal{M})}$ . Using a coarea formula for  $\|u \circ R_{\text{cp}}\|_{\mathcal{H}^k(\Omega_\delta)}$  in the tangential and normal directions of  $\mathcal{M}$ , the desired scale factor  $\delta^{r/2}$  arises from the volume of the hypersphere with radius  $\delta$  in  $\mathbb{R}^r$ .  $\square$

**3. Partial differential equations on  $\mathcal{M}$ .** In this section, we prove Theorem 1.1. Let  $I_d$  denote the identity matrix of size  $d \times d$ . Using the matrix of unit normal bases  $N(p)$  in (2.1), we define the orthogonal projector

$$\mathcal{P} := \mathcal{P}(p) = I_d - N(p)N(p)^T, \quad (3.1)$$

which projects vectors from  $\mathbb{R}^d$  at  $p \in \mathcal{M}$  onto the tangent space  $\mathcal{T}_p\mathcal{M}$ . We denote columns of  $\mathcal{P}$  by  $\mathcal{P}_i$ , whose entries are given by  $\mathcal{P}_{ij}$  with  $i, j = 1, 2, \dots, d$ . We remark that, it is not required in [33] that the bases in (2.1) be mutually orthogonal. In this case, the transpose  $T$  in (3.1) should be replaced by a pseudoinverse  $\dagger$ .

Let  $\nabla$  be the gradient operator and  $\Delta$  be the Laplacian operator in  $\mathbb{R}^d$ . The gradient operator on  $\mathcal{M}$  is defined as

$$\nabla_{\mathcal{M}} := \mathcal{P}\nabla, \quad (3.2)$$

and the Laplace-Beltrami operator is defined as [10]

$$\Delta_{\mathcal{M}} := \nabla_{\mathcal{M}} \cdot \nabla_{\mathcal{M}} = (\mathcal{P}\nabla) \cdot (\mathcal{P}\nabla). \quad (3.3)$$

Using definitions (3.2) and (3.3), we completely define the elliptic operator  $\mathcal{L}_{\mathcal{M}}$  in (1.1). We now make the necessary assumption about this manifold PDE.

A2. *Assume that  $\mathcal{L}_{\mathcal{M}}$  in (1.1) is a second-order strongly elliptic operator whose coefficients are in  $\mathcal{W}_\infty^{m-2}(\mathcal{M})$  and (1.1) admits a classical solution  $u^* \in \mathcal{H}^m(\mathcal{M})$  for some  $m \geq 2$ .*

Using the restriction map  $R_{\text{cp}}$  in (2.2), the manifold operator  $\mathcal{L}_{\mathcal{M}}$  can be embedded to  $\Omega_{\delta}$  by [34]

$$\mathcal{L}_E := -(a \circ R_{\text{cp}})\Delta + (\vec{b} \circ R_{\text{cp}}) \cdot \nabla + (c \circ R_{\text{cp}}). \quad (3.4)$$

The coefficients in (3.4) are obtained from those in (1.1) by the constant-along-normal extension. With the use of some carefully chosen  $\delta$  and the trial centers, this embedding technique allows the development of extrinsic formulations. First, we need a *regularity estimate* that holds in Sobolev spaces. We extend the results in [8, Thm. 3.2] to codimension  $r \geq 1$  as below.

**LEMMA 3.1.** *Suppose that A1 and A2 hold. Let  $\Omega_{\delta}$  be an embedding domain as in (2.3) with some  $\delta < \delta_{\mathcal{M}}$ . Then, for any  $u \in \mathcal{H}^m(\mathcal{M})$ , the inequality*

$$\|u\|_{\mathcal{H}^k(\mathcal{M})} \leq C\delta^{-r/2} \|\mathcal{L}_E(u \circ R_{\text{cp}})\|_{\mathcal{H}^{k-2}(\Omega_{\delta})}, \quad 2 \leq k \leq m,$$

holds with some constant  $C$  depending only on  $\mathcal{M}$  and  $k$ .

**PROOF.** For any  $u \in \mathcal{H}^m(\mathcal{M})$ , applying an elliptic Neumann-boundary regularity estimate [50] to the operator  $\mathcal{L}_E$  and the function  $u \circ R_{\text{cp}}$  yields

$$\|u \circ R_{\text{cp}}\|_{\mathcal{H}^k(\Omega_{\delta})} \leq C_{\Omega_{\delta},k} \left( \|\mathcal{L}_E(u \circ R_{\text{cp}})\|_{\mathcal{H}^{k-2}(\Omega_{\delta})} + \|\partial_{\vec{n}}(u \circ R_{\text{cp}})\|_{\mathcal{H}^{k-3/2}(\partial\Omega_{\delta})} \right).$$

The domain-dependent constant can be bounded as  $C_{\Omega_{\delta},k} \leq C_{\Omega_{\mathcal{M}},k} = C_{\mathcal{M},k}$ . By Lemma 2.1, we can bound  $\|u \circ R_{\text{cp}}\|_{\mathcal{H}^k(\Omega_{\delta})}$  from below via using  $\delta^{r/2}\|u\|_{\mathcal{H}^k(\mathcal{M})}$ . The constant-along-normal property of  $u \circ R_{\text{cp}}$  ensures that  $\partial_{\vec{n}}(u \circ R_{\text{cp}}) = 0$  on  $\partial\Omega_{\delta}$  and the proof is completed.  $\square$

**3.1. Kernels and discrete settings.** We are ready to work in trial spaces. Given any discrete set of points  $\Xi \subset \mathcal{M}$ , let  $\text{dist}_{\Omega} := \|\cdot\|_2$  and  $\text{dist}_{\mathcal{M}}$  be the Euclidean and geodesic measures in  $\Omega$  and on  $\mathcal{M}$  respectively. For  $\Pi \in \{\Omega_{\delta}, \mathcal{M}\}$ , the *fill distance*  $h_{\Xi,\Pi}$  and the *separation distance*  $q_{\Xi,\Pi}$  are defined as

$$h_{\Xi,\Pi} := \sup_{\zeta \in \Pi} \inf_{\eta \in \Xi} \text{dist}_{\Pi}(\zeta, \eta), \quad \text{and} \quad q_{\Xi,\Pi} := \frac{1}{2} \inf_{\eta^i \neq \eta^j \in \Xi} \text{dist}_{\Pi}(\eta^i, \eta^j), \quad (3.5)$$

respectively. In Theorem 1.1, the *mesh ratio* of the set  $\Xi$  is defined as

$$\rho_{\Xi,\Pi} := h_{\Xi,\Pi}/q_{\Xi,\Pi}. \quad (3.6)$$

For brevity, we use  $h_{\Xi} = h_{\Xi,\mathcal{M}}$ ,  $q_{\Xi} = q_{\Xi,\mathcal{M}}$  and  $\rho_{\Xi} = \rho_{\Xi,\mathcal{M}}$  later, unless otherwise stated.

For discretization, our proposed least-squares methods require two sets on the manifold.

**A3.** *Let  $X = \{x^1, \dots, x^{n_x}\} \subset \mathcal{M}$  and  $Z = \{z^1, \dots, z^{n_z}\} \subset \mathcal{M}$  be the sets of collocation points and trial centers, respectively. We assume both of them are quasi-uniform, that is, both admissible point sets satisfy*

$$q_{\Xi} \leq h_{\Xi} \leq \rho_{\Xi} q_{\Xi}, \quad \Xi \in \{X, Z\} \quad (3.7)$$

for some constants  $\rho_{\Xi} \geq 1$ .

Instead of working with arbitrary manifold kernels  $\Psi_m$ , we focus on those related to some global kernels  $\Phi_\tau : \mathbb{R}^d \times \mathbb{R}^d \rightarrow \mathbb{R}$  that are symmetric positive definite with Fourier transforms  $\hat{\Phi}_\tau$  satisfying the following decay

$$c_1(1 + \|\omega\|_2^2)^{-\tau} \leq \hat{\Phi}_\tau(\omega) \leq c_2(1 + \|\omega\|_2^2)^{-\tau}, \quad \text{for all } \omega \in \mathbb{R}^d, \quad (3.8)$$

for some constants  $0 < c_1 \leq c_2$ . From [35], these  $\Phi_\tau$  reproduce  $\mathcal{H}^\tau(\mathbb{R}^d)$  for any  $\tau > d/2$ . One example of such kernels is the standard Whittle-Matérn-Sobolev kernels [35],

$$\Phi_\tau(x, y) := \frac{\|x - y\|_2^{\tau-d/2} \mathcal{K}_{\tau-d/2}(\|x - y\|_2)}{2^{\tau-1} \Gamma(\tau)}, \quad (3.9)$$

where  $\mathcal{K}$  is the Bessel functions of the second kind. The class of Wendland compactly supported kernels is another example [51]. Simply by restricting such global kernels  $\Phi_\tau$  on  $\mathcal{M}$ , we can obtain restricted kernels  $\Psi_m : \mathcal{M} \times \mathcal{M} \rightarrow \mathbb{R}$  that reproduce  $\mathcal{H}^m(\mathcal{M})$  under the following assumption [13, 38].

A4. Let  $m = \tau - r/2 > d_{\mathcal{M}}/2$ . Suppose that the kernel  $\Psi_m : \mathcal{M} \times \mathcal{M} \rightarrow \mathbb{R}$  takes the form of

$$\Psi_m(\cdot, \cdot) := \Phi_\tau(\cdot, \cdot)|_{\mathcal{M} \times \mathcal{M}}, \quad (3.10)$$

for some kernel  $\Phi_\tau : \mathbb{R}^d \times \mathbb{R}^d \rightarrow \mathbb{R}$  that satisfies (3.8).

**3.2. Stability and consistency.** We prove a stability estimate on  $\mathcal{M}$ , as well as a theorem of consistency for arbitrary codimensions in this section. Firstly, the sampling inequality in [8, Thm. 3.3] should be extended to arbitrary codimensions.

LEMMA 3.2. Suppose that A1–A3 hold. Let  $\Omega_\delta$  be an embedding domain defined as that in (2.3) with some  $\delta = h_X < \delta_{\mathcal{M}}$ . Further assume that the set of collocation points  $X \subset \mathcal{M}$  is sufficiently dense. Then, for any integer  $k$  with  $2 \leq k \leq m$ ,

$$\|\mathcal{L}_E(u \circ R_{\text{cp}})\|_{\mathcal{H}^{k-2}(\Omega_\delta)} \leq C\delta^{\tau/2} \left( h_X^{m-k} \|u\|_{\mathcal{H}^m(\mathcal{M})} + h_X^{d_{\mathcal{M}}/2-k+2} \|\mathcal{L}_{\mathcal{M}}u\|_{\ell_2(X)} \right)$$

holds for all  $u \in \mathcal{H}^m(\mathcal{M})$  and some positive constant  $C$  depending only on  $\mathcal{M}$ ,  $\mathcal{L}_{\mathcal{M}}$ ,  $m$  and  $k$ .

PROOF. Applying a sampling inequality [9, Lem. 3.1] to  $\mathcal{L}_E(u \circ R_{\text{cp}}) \in \mathcal{H}^{m-2}(\Omega_\delta)$  at some sufficiently dense set  $X \subset \mathcal{M}$ , we have

$$\begin{aligned} & \|\mathcal{L}_E(u \circ R_{\text{cp}})\|_{\mathcal{H}^{k-2}(\Omega_\delta)} \\ & \leq C_{\Omega_\delta, k, m} \left( h_{X, \Omega_\delta}^{m-k} \|\mathcal{L}_E(u \circ R_{\text{cp}})\|_{\mathcal{H}^{m-2}(\Omega_\delta)} + h_{X, \Omega_\delta}^{d_{\mathcal{M}}/2-k+2} \|\mathcal{L}_E(u \circ R_{\text{cp}})\|_{\ell_2(X)} \right), \end{aligned} \quad (3.11)$$

in which the constant  $C_{\Omega_\delta, m, k}$  can be bounded by another constant  $C_{\Omega_{\mathcal{M}}, m, k}$ .

Since  $\mathcal{M}$  is smooth and compact, by [13, Thm. 6], the measures on  $\mathcal{M}$  and in  $\Omega_\delta$  are proportional with respect to some constants depending on the diameter of  $\mathcal{M}$ , i.e.,  $\text{dist}_{\mathcal{M}}(x, y) \sim \|x - y\|_2$ . Note that any  $\zeta \in \Omega_\delta$  can be decomposed to  $\zeta = R_{\text{cp}}(\zeta) + t\vec{n}$  by some unit normal vector  $\vec{n}$  at the point  $R_{\text{cp}}(\zeta) \in \mathcal{M}$  and  $t \in [0, \delta]$ ; we can see that

$$\begin{aligned} h_{X, \Omega_\delta}^2 & := \sup_{\zeta \in \Omega_\delta} \inf_{\eta \in X} \|\zeta - \eta\|_2^2 \leq \sup_{\zeta \in \Omega_\delta} \inf_{\eta \in X} \|R_{\text{cp}}(\zeta) - \eta\|_2^2 + \delta^2 \\ & \sim \sup_{y \in \mathcal{M}} \inf_{\eta \in X} \text{dist}_{\mathcal{M}}^2(y, \eta) + \delta^2. \end{aligned}$$

In other words, by choosing  $\delta = h_{X,\mathcal{M}}$ , we have proportional fill distances  $h_{X,\Omega_\delta} \sim h_{X,\mathcal{M}}$  with some constant depending on  $\mathcal{M}$ .

Applying [17, Lem. 3.4] and Lemma 2.1 yields an upper bound for the first term on the right of (3.11), i.e.,

$$\begin{aligned} \|\mathcal{L}_E(u \circ R_{\text{cp}})\|_{\mathcal{H}^{m-2}(\Omega_\delta)} &\leq C_{\Omega,\mathcal{M},\mathcal{L}_E} \|u \circ R_{\text{cp}}\|_{\mathcal{H}^m(\Omega_\delta)} \\ &\leq C_{\Omega,\mathcal{M},\mathcal{L}_E} C_{\mathcal{M},m} \delta^{r/2} \|u\|_{\mathcal{H}^m(\mathcal{M})}. \end{aligned}$$

By A2, there exists some constant  $C_{\mathcal{M},\mathcal{L}_E,m}$  that can bound  $C_{\Omega,\mathcal{M},\mathcal{L}_E} C_{\mathcal{M},m}$  from the above. Together, we have

$$\begin{aligned} &\|\mathcal{L}_E(u \circ R_{\text{cp}})\|_{\mathcal{H}^{k-2}(\Omega_\delta)} \\ &\leq C_{\mathcal{M},\mathcal{L}_E,k,m} \left( h_X^{m-k} \delta^{r/2} \|u\|_{\mathcal{H}^m(\mathcal{M})} + h_X^{d/2-k+2} \|\mathcal{L}_E(u \circ R_{\text{cp}})\|_{\ell_2(X)} \right) \\ &\sim C_{\mathcal{M},\mathcal{L}_E,k,m} \delta^{r/2} \left( h_X^{m-k} \|u\|_{\mathcal{H}^m(\mathcal{M})} + h_X^{(d-r)/2-k+2} \|\mathcal{L}_E(u \circ R_{\text{cp}})\|_{\ell_2(X)} \right). \end{aligned}$$

The lemma follows from  $d_{\mathcal{M}} = d - r$ .  $\square$

LEMMA 3.3. *Suppose that A1–A3 hold for some integers  $m > d_{\mathcal{M}}/2$  and  $2 \leq k \leq m$ . Then there exists some constant  $C$  depending only on  $\mathcal{M}$ ,  $\mathcal{L}_{\mathcal{M}}$ ,  $m$  and  $k$  such that*

$$\|u\|_{\mathcal{H}^k(\mathcal{M})} \leq C h_X^{d_{\mathcal{M}}/2-k+2} \|\mathcal{L}_{\mathcal{M}} u\|_{\ell_2(X)} \quad (3.12)$$

holds for all trial functions  $u \in \mathcal{U}_Z$  as in (1.2), provided that the sets of trial centers  $Z$  and collocation points  $X$  satisfy

$$C_{\mathcal{M},\mathcal{L}_{\mathcal{M}},\Psi_m,\rho_Z,k} h_X^{m-k} h_Z^{-m} \|u\|_{L^2(\mathcal{M})} < \frac{1}{2} \|u\|_{\mathcal{H}^k(\mathcal{M})} \quad (3.13)$$

for some constant  $C_{\mathcal{M},\mathcal{L}_{\mathcal{M}},\Psi_m,\rho_Z,k} > 0$  independent of  $X$ .

PROOF. By combining Lemmas 3.1 and 3.2 with a sufficiently small  $\delta = h_X < \delta_{\mathcal{M}}$ , a stability estimate can be arrived

$$\|u\|_{\mathcal{H}^k(\mathcal{M})} \leq C_{\mathcal{M},\mathcal{L}_{\mathcal{M}},m,k} \left( h_X^{m-k} \|u\|_{\mathcal{H}^m(\mathcal{M})} + h_X^{d_{\mathcal{M}}/2-k+2} \|\mathcal{L}_{\mathcal{M}} u\|_{\ell_2(X)} \right), \quad (3.14)$$

for  $m \geq k \geq 2$ . By A1 for  $\mathcal{M}$ , we can apply an inverse inequality [20, Thm. 10] for trial functions  $u \in \mathcal{U}_Z$ , i.e.,

$$\|u\|_{\mathcal{H}^m(\mathcal{M})} \leq C_{\mathcal{M},\Psi_m,\rho_Z} h_Z^{-m} \|u\|_{L^2(\mathcal{M})}. \quad (3.15)$$

Putting (3.15) into (3.14) completes the proof.  $\square$

The oversampling requirement in (3.13) specifies the condition on the denseness of  $X$  with respect to  $Z$  that can ensure stability. A sufficient condition to satisfy (3.13) is by taking  $h_X^{m-k} h_Z^{-m} < 1/2$ , which, however, may be unnecessary – as the numerical experiments in Section 5 indicate.

The last piece of the technical details we need is about consistency that can be obtained by using convergence estimates for kernel-based interpolation on manifolds [13, Thm. 11].

LEMMA 3.4. *Suppose that A1 and A2 hold for some  $m \geq 2 + d_{\mathcal{M}}/2$ . Then, for any  $u \in \mathcal{H}^m(\mathcal{M})$ , we have*

$$\|\mathcal{L}_{\mathcal{M}} u\|_{L^\infty(\mathcal{M})} \leq C \|u\|_{W_\infty^2(\mathcal{M})}, \quad (3.16)$$

with some constant  $C$  depending on  $\mathcal{M}$  and  $\mathcal{L}_{\mathcal{M}}$ .

PROOF. By a Sobolev embedding theorem [2, Prop.2.2], we know  $u \in \mathcal{W}_{\infty}^2(\mathcal{M})$ . We pick a sufficiently small  $\delta < \delta_{\mathcal{M}}$  so that  $R_{\text{cp}}(x)$  is of class  $\mathcal{C}^m$  in  $\Omega_{\delta}$ . Due to the boundedness of the coefficients in  $\mathcal{L}_{\mathcal{M}}$ , we have [17]

$$\begin{aligned} \|\mathcal{L}_{\mathcal{M}}u\|_{L^{\infty}(\mathcal{M})} &\leq \|\mathcal{L}_E(u \circ R_{\text{cp}})\|_{L^{\infty}(\Omega_{\delta})} \leq C_{\mathcal{M}, \mathcal{L}_{\mathcal{M}}} \|u \circ R_{\text{cp}}\|_{\mathcal{W}_{\infty}^2(\Omega_{\delta})} \\ &= C_{\mathcal{M}, \mathcal{L}_{\mathcal{M}}} \max_{|\alpha| \leq 2} \text{ess sup}_{x \in \Omega_{\delta}} \left| D_x^{\alpha} \{u \circ R_{\text{cp}}\} \right|. \end{aligned} \quad (3.17)$$

Using the fact that  $\mathcal{M}$  has bounded geometry, applying chain rule yields  $\left| D_x^{\alpha} \{u \circ R_{\text{cp}}\} \right| \leq C_{\alpha, \mathcal{M}} \|u\|_{\mathcal{W}_{\infty}^2(\mathcal{M})}$  for any  $x \in \Omega_{\delta}$  and  $|\alpha| \leq m$ . Taking the maximum of all  $C_{\alpha, \mathcal{M}}$  with  $|\alpha| \leq 2$  yields (3.16).  $\square$

LEMMA 3.5. *Suppose that A1–A4 hold. Let  $I_Z u^*$  be the interpolant of  $u^*$  from the trial space  $\mathcal{U}_Z$  as in (1.2). Then*

$$\inf_{u \in \mathcal{U}_Z} \|\mathcal{L}_{\mathcal{M}}u - \mathcal{L}_{\mathcal{M}}u^*\|_{\ell_2(X)} \leq \|\mathcal{L}_{\mathcal{M}}(I_Z u^*) - \mathcal{L}_{\mathcal{M}}u^*\|_{\ell_2(X)} \quad (3.18)$$

$$\leq Ch_X^{-d_{\mathcal{M}}/2} h_Z^{m-d_{\mathcal{M}}/2-2} \|u^*\|_{\mathcal{H}^m(\mathcal{M})} \quad (3.19)$$

holds for some constant  $C$  depending only on  $\mathcal{M}, \Psi_m, \mathcal{L}_{\mathcal{M}}$  and  $\rho_X$ .

PROOF. Since the interpolant  $I_Z u^* \in \mathcal{U}_Z$  of  $u^*$  is a feasible solution to the minimization problem, the inequality (3.18) is trivial. By Lemma 3.4 and an error estimate for kernel-based interpolation on manifolds [13, Cor.13], we have

$$\begin{aligned} \|\mathcal{L}_{\mathcal{M}}(I_Z u^*) - \mathcal{L}_{\mathcal{M}}u^*\|_{\ell_2(X)} &\leq n_X^{1/2} \|\mathcal{L}_{\mathcal{M}}(I_Z u^*) - \mathcal{L}_{\mathcal{M}}u^*\|_{L^{\infty}(\mathcal{M})} \\ &\leq C_{\mathcal{M}, \mathcal{L}_{\mathcal{M}}} n_X^{1/2} \|I_Z u^* - u^*\|_{\mathcal{W}_{\infty}^2(\mathcal{M})} \\ &\leq C_{\mathcal{M}, \Psi_m, \mathcal{L}_{\mathcal{M}}} q_X^{-d_{\mathcal{M}}/2} h_Z^{m-d_{\mathcal{M}}/2-2} \|u^*\|_{\mathcal{H}^m(\mathcal{M})}, \end{aligned}$$

provided that  $m \geq \lceil 3 + d_{\mathcal{M}}/2 \rceil$  as required in [13]. We arrive at (3.19) by the fact that  $X$  is  $\rho_X$ -uniform.  $\square$

PROOF (Theorem 1.1). We consider the approximation error in two parts:

$$\|U_{X,Z} - u^*\|_{\mathcal{H}^k(\mathcal{M})} \leq \|U_{X,Z} - I_Z u^*\|_{\mathcal{H}^k(\mathcal{M})} + \|I_Z u^* - u^*\|_{\mathcal{H}^k(\mathcal{M})}. \quad (3.20)$$

By the stability estimate in Lemma 3.3, we can bound the first term on the right side of (3.20) by

$$\|U_{X,Z} - I_Z u^*\|_{\mathcal{H}^k(\mathcal{M})} \leq C_{\mathcal{M}, \mathcal{L}_{\mathcal{M}}, m, k} h_X^{d_{\mathcal{M}}/2-k+2} \|\mathcal{L}_{\mathcal{M}}(U_{X,Z} - I_Z u^*)\|_{\ell_2(X)}.$$

By (3.18), we obtain

$$\begin{aligned} \|\mathcal{L}_{\mathcal{M}}(U_{X,Z} - I_Z u^*)\|_{\ell_2(X)} &\leq \|\mathcal{L}_{\mathcal{M}}(U_{X,Z} - u^*)\|_{\ell_2(X)} + \|\mathcal{L}_{\mathcal{M}}(u^* - I_Z u^*)\|_{\ell_2(X)} \\ &\leq 2\|\mathcal{L}_{\mathcal{M}}(u^* - I_Z u^*)\|_{\ell_2(X)}. \end{aligned}$$

Then, the consistency estimate in Lemma 3.5 suggests that

$$\begin{aligned} \|U_{X,Z} - I_Z u^*\|_{\mathcal{H}^k(\mathcal{M})} &\leq 2C_{\mathcal{M}, \mathcal{L}_{\mathcal{M}}, m, k} h_X^{d_{\mathcal{M}}/2-k+2} \|\mathcal{L}_{\mathcal{M}}(u^* - I_Z u^*)\|_{\ell_2(X)} \\ &\leq 2C_{\mathcal{M}, \mathcal{L}_{\mathcal{M}}, \Psi_m, \rho_X} h_X^{-k+2} h_Z^{m-d_{\mathcal{M}}/2-2} \|u^*\|_{\mathcal{H}^m(\mathcal{M})}. \end{aligned}$$

For  $m \geq \lceil k + 1 + d_{\mathcal{M}}/2 \rceil$ , we can use the convergence estimate in [13, Cor.13] to bound the other term in (3.20) as follows:

$$\begin{aligned} \|I_Z u^* - u^*\|_{\mathcal{H}^k(\mathcal{M})} &\leq C_{\mathcal{M}} \|I_Z u^* - u^*\|_{\mathcal{W}_{\infty}^k(\mathcal{M})} \\ &\leq C_{\mathcal{M}, \Psi_m, k} h_Z^{m-k-d_{\mathcal{M}}/2} \|u^*\|_{\mathcal{H}^m(\mathcal{M})}. \end{aligned}$$

Combining these two upper bounds yields the desired error estimate.  $\square$

**4. Extrinsic meshless collocation methods and implementation.** For numerical computation of the least-squares solution  $U_{X,Z}$  in (1.3), we must find means to evaluate the term  $\mathcal{L}_{\mathcal{M}}u$ . In this section, we present analytical and approximate expressions of differentiation of the projector in (3.1). The latter completely avoid differentiating the projector in (3.1), which is suitable when such information is unavailable.

**4.1. Kansa-type Projection Method.** If analytical information about the derivatives of the projector  $\mathcal{P}$  in (3.1) are available, it is possible to analytically transform  $\mathcal{L}_{\mathcal{M}}$  in (1.1) into the standard Cartesian coordinates. First, the manifold gradient form of  $u$ , see (3.2), can be expanded as

$$\nabla_{\mathcal{M}}u = \mathcal{P}\nabla u = \begin{bmatrix} \mathcal{P}_1 \cdot \nabla \\ \vdots \\ \mathcal{P}_d \cdot \nabla \end{bmatrix} u, \quad (4.1)$$

where  $\mathcal{P}_k$  is the  $k$ th column of  $\mathcal{P}$ . Similarly, we can get the extrinsic formula of the Laplace-Beltrami operator from its definition (3.3) as

$$\begin{aligned} \Delta_{\mathcal{M}}u &= (\mathcal{P}\nabla) \cdot (\mathcal{P}\nabla)u \\ &= \text{trace}(\mathcal{P} \cdot J(\nabla_{\mathcal{M}}u)^T) \\ &= \sum_{i=1}^d \left( \zeta_i \frac{\partial u}{\partial x_i} + \mathcal{P}_{ii} \frac{\partial^2 u}{\partial x_i^2} \right) + \sum_{\substack{i,j=1 \\ i \neq j}}^d \mathcal{P}_{ij} \frac{\partial^2 u}{\partial x_i \partial x_j}, \end{aligned} \quad (4.2)$$

with coefficients  $\zeta_i = \text{trace}(\mathcal{P} \cdot J(\mathcal{P}_i)^T)$ , for  $i = 1, \dots, d$ , where  $\mathcal{P}_{ij}$  denotes the  $ij$ -th entry of  $\mathcal{P}$  and  $J$  is the Jacobian operator. Using (4.1) and (4.2), we can transform the operator in (1.1) into a collocation-ready form

$$\mathcal{L}_{\mathcal{M}} = -a \left( \sum_{i=1}^d \left( \zeta_i \frac{\partial}{\partial x_i} + \mathcal{P}_{ii} \frac{\partial^2}{\partial x_i^2} \right) + \sum_{\substack{i,j=1 \\ i \neq j}}^d \mathcal{P}_{ij} \frac{\partial^2}{\partial x_i \partial x_j} \right) + \sum_{k=1}^d b_k (\mathcal{P}_k \cdot \nabla) + c. \quad (4.3)$$

A simple demonstration of such a transformation is given below.

**Example.** Let  $\mathcal{M} \in \mathbb{R}^3$  be the unit sphere. We consider the differential operator  $\mathcal{L}_{\mathcal{M}} = \Delta_{\mathcal{M}} - \vec{1} \cdot \nabla_{\mathcal{M}}$ . Firstly, we compute the orthogonal projection operator

$$\mathcal{P} = \begin{bmatrix} -x^2 + 1 & -xy & -xz \\ -xy & -y^2 + 1 & -yz \\ -xz & -yz & -z^2 + 1 \end{bmatrix}.$$

Simplifying with the fact that  $x^2 + y^2 + z^2 = 1$ , we get the coefficients in (4.2):  $(\zeta_1, \zeta_2, \zeta_3) = (-2x, -2y, -2z)$ . Putting these coefficients into (4.3), we now express the surface operator entirely in Cartesian coordinates as

$$\begin{aligned} \mathcal{L}_{\mathcal{M}} = & \left( (x-1)^2 + x(y+z) - 2 \right) \frac{\partial}{\partial x} + \left( (y-1)^2 + y(x+z) - 2 \right) \frac{\partial}{\partial y} \\ & + \left( (z-1)^2 + z(x+y) - 2 \right) \frac{\partial}{\partial z} \\ & + \left( -x^2 + 1 \right) \frac{\partial^2}{\partial x^2} + \left( -y^2 + 1 \right) \frac{\partial^2}{\partial y^2} + \left( -z^2 + 1 \right) \frac{\partial^2}{\partial z^2} \\ & - 2xy \frac{\partial^2}{\partial x \partial y} - 2xz \frac{\partial^2}{\partial x \partial z} - 2yz \frac{\partial^2}{\partial y \partial z}, \end{aligned}$$

which no longer has any implicit dependency on  $\mathcal{M}$  and can be used for collocation. Note that, for the unit sphere,  $\Delta_{\mathcal{M}}$  in (3.3) is the standard Laplacian-Beltrami in the spherical polar coordinates. Because its canonical metric of sectional curvature is constant when the radius is.  $\square$

In the coming section, we deal with the situation, in which the derivatives of  $\mathcal{P}$  are not available analytically.

**4.2. Approximated Kansa Method.** We adopt the meshless approach in [15] to approximate the gradient of a function  $u \in \mathcal{H}^m(\mathcal{M})$  based on its unknown nodal values  $u(Z)$  at some given set of trial centers  $Z = \{z^1, \dots, z^{n_z}\} \subset \mathcal{M}$ . We use the restricted kernels  $\Psi_m$  that satisfy A4 and can reproduce  $\mathcal{H}^m(\mathcal{M})$ . Let  $\Psi_m(Z, Z)$  with  $ij$ -entry  $\Psi_m(z^i, z^j)$  be the interpolation matrix of  $\Psi_m$  on  $Z$ . The approximate interpolant  $I_Z u$  in the trial space  $\mathcal{U}_Z$  in (1.2) can then be expressed by a linear expansion

$$I_Z u = [\Psi_m(\cdot, Z)][\Psi_m(Z, Z)]^{-1} u(Z). \quad (4.4)$$

Via (4.4), we define an approximate manifold gradient operator by

$$\tilde{\nabla}_{\mathcal{M}} u := \nabla_{\mathcal{M}}(I_Z u) = \begin{bmatrix} \mathcal{P}_1 \cdot \nabla \\ \vdots \\ \mathcal{P}_d \cdot \nabla \end{bmatrix} (I_Z u),$$

in which the gradient operator acts upon the variable of  $\Psi_m(\cdot, Z)$ . Thus, by using the notation in [15], the  $k$ th component, for  $1 \leq k \leq d$ , of  $\tilde{\nabla}_{\mathcal{M}} u$  is given by

$$[\tilde{\nabla}_{\mathcal{M}} u]_k = G_k(\cdot, Z) u(Z) := \left( \mathcal{P}_k^T [\nabla \Psi_m(\cdot, Z)][\Psi_m(Z, Z)]^{-1} \right) u(Z), \quad (4.5)$$

where  $G_k(\cdot, Z) : \mathcal{M} \rightarrow \mathbb{R}^{1 \times n_z}$  is a row-vector function that can be evaluated at any point on the manifold. For the sake of direct collocation, we require the values  $\tilde{\nabla}_{\mathcal{M}} u(X)$ .

To approximate the manifold Laplacian without using any derivative of  $\mathcal{P}$ , we apply a similar pseudospectral technique to approximate the manifold divergence of  $I_Z(\tilde{\nabla}_{\mathcal{M}} u)$ , whose  $k$ th component is the expression  $I_Z[\tilde{\nabla}_{\mathcal{M}} u]_k$  of  $[\tilde{\nabla}_{\mathcal{M}} u]_k$  from  $\mathcal{U}_Z$ . We define an approximate Laplace-Beltrami operator as

$$\tilde{\Delta}_{\mathcal{M}} u := \tilde{\nabla}_{\mathcal{M}} \cdot \tilde{\nabla}_{\mathcal{M}} u = \nabla_{\mathcal{M}} \cdot \begin{bmatrix} I_Z[\tilde{\nabla}_{\mathcal{M}} u]_1 \\ \vdots \\ I_Z[\tilde{\nabla}_{\mathcal{M}} u]_d \end{bmatrix}.$$

To simplify, we consider the interpolation operator in matrix form as that in (4.4) to yield

$$\tilde{\Delta}_{\mathcal{M}}u = (\mathcal{P}_1^T \nabla, \dots, \mathcal{P}_d^T \nabla) \cdot \begin{bmatrix} [\Psi_m(\cdot, Z)][\Psi_m(Z, Z)]^{-1} [[\tilde{\nabla}_{\mathcal{M}}u]_1(Z)] \\ \vdots \\ [\Psi_m(\cdot, Z)][\Psi_m(Z, Z)]^{-1} [[\tilde{\nabla}_{\mathcal{M}}u]_d(Z)] \end{bmatrix}. \quad (4.6)$$

Using (4.5), we can rewrite (4.6) as

$$\tilde{\Delta}_{\mathcal{M}}u = \sum_{k=1}^d G_k(\cdot, Z)G_k(Z, Z)u(Z).$$

Finally, we arrive at an approximation to (1.1), which allows collocation at any point on  $\mathcal{M}$  by

$$\tilde{\mathcal{L}}_{\mathcal{M}}u = \left( a \sum_{k=1}^d G_k(\cdot, Z)G_k(Z, Z) + \vec{b}^T G(\cdot, Z) + c[\Psi_m(\cdot, Z)][\Psi_m(Z, Z)]^{-1} \right) u(Z). \quad (4.7)$$

Equation (4.7) allows us to assemble the collocation matrix system either in terms of nodal values  $u(Z)$  or expansion coefficients  $\lambda_Z := [\Psi_m(Z, Z)]^{-1}u(Z)$ .

Note that when  $X = Z$ , the projection method developed by [15] is identical to our approximated algorithm. It was proved that

$$\|\mathcal{L}_{\mathcal{M}}u - \tilde{\mathcal{L}}_{\mathcal{M}}u\|_{L^2(\mathcal{M})} = \mathcal{O}(\rho_Z h_Z^{m-2})$$

for  $m > 2.5 + d_{\mathcal{M}}/2$  and sufficiently dense  $Z$ . Going from the square approach to our least-squares one not only allows us to obtain error estimates for the numerical solution, but also provides extra flexibility in the distribution of data points. In the coming section, we will demonstrate that having more collocation points (i.e., more information of the PDE) indeed helps find better approximate solutions from the trial space.

**5. Numerical demonstrations.** In this section, we numerically test the proposed extrinsic meshless collocation methods.

We focus on  $\mathcal{H}^2(\mathcal{M})$  convergent methods, i.e.,  $k = 2$  in Theorem 1.1, and use restricted Whittle-Matérn Sobolev kernels given by (3.9) and (3.10) with various orders  $m \geq \lceil 3 + d_{\mathcal{M}}/2 \rceil$  of smoothness. Both sets of trial centers  $Z$  and collocation points  $X$  are scattered and quasi-uniform on  $\mathcal{M}$ . For one-dimensional cases, they are equally-spaced on the curve. For two-dimensional surfaces, data points were generated by using the algorithm in [43]. In cases when fill distances are not immediately available, we do not compute them in order to avoid unnecessary computational overhead. Instead, we use the fact that data points are quasi-uniform and use the total numbers of points as variables, i.e.,  $h_X/h_Z \sim (n_Z/n_X)^{1/d_{\mathcal{M}}}$ , to control the ratio between fill distances.

In our implementation, we seek for the least-squares minimizer of (1.3) in the form of

$$u = [\Psi_m(\cdot, Z)]\lambda_Z \in \mathcal{U}_Z$$

in terms of its expansion coefficients  $\lambda_Z \in \mathbb{R}^{n_Z}$ . For the Kansa-type Projection Method (KPM) in Section 4.1, we directly collocate  $\mathcal{L}_{\mathcal{M}}u$  via (4.3) at  $X$  to obtain

$$\mathcal{L}_{\mathcal{M}}u(X) = [\mathcal{L}_{\mathcal{M}}\Psi_m(X, Z)]\lambda_Z = f(X),$$

TABLE 1

Comparison of computational time(s) among  $KEM_2$ , our  $KPM_2$ , and  $AKM_2$  by using various  $n_X \approx 2n_Z$ , under the same settings as in Figure 1.

$n_Z$	223	179	144	116	93
$h_Z$	0.0282	0.0351	0.0437	0.0545	0.0679
$KEM_2$	2.5565	1.4367	0.8713	0.6213	0.3833
$KPM_2$	0.8828	0.4571	0.3289	0.2732	0.2097
$AKM_2$	0.5142	0.3078	0.2499	0.1886	0.1626

where  $\mathcal{L}_{\mathcal{M}}u(X)$  is a vector of size  $n_X$  and the matrix  $[\mathcal{L}_{\mathcal{M}}\Psi_m(X, Z)]$  is  $n_X \times n_Z$ . For the Approximated Kansa Method (AKM) in Section 4.2, we use nodal values (but it's  $\lambda_Z$  below) of the approximation in (4.7) at  $X$  to obtain the following:

$$\tilde{\mathcal{L}}_{\mathcal{M}}u(X) = [\tilde{\mathcal{L}}_{\mathcal{M}}\Psi_m(X, Z)]\lambda_Z = f(X).$$

Both systems of equations are solved by a direct QR-based solver.

In Section 5.1, we present two convergence studies on modified Helmholtz equations on manifolds with  $d_{\mathcal{M}} = 1$ . We compare the resulting errors obtained by our methods (KPM and AKM) with those by others in literatures under different oversampling strategies. Next, in Section 5.2, we study the proposed approaches with two examples in  $\mathbb{R}^3$  with  $d_{\mathcal{M}} = 2$ . The first test aims to further verify the convergence of KPM under different linear ratios of oversampling. In the second test, we numerically compare the performance between oversampled KPM and AKM. Lastly, we end this section with some simulations of reaction diffusion equations in Section 5.3.

**5.1. Effects of oversampling.** We now compare the proposed methods with a kernel-based embedding method (KEM) in [8]. Various oversampling strategies are examined; subscript 1 and 2 indicates linear ratio of oversampling with  $X = Z$  (no oversampling) and  $n_X \approx 2n_Z$ , respectively. The sufficient ratio  $h_X \sim h_Z^3$ , which ensures the stability in Lemma 3.3, is indicated by subscript  $c$ .

We consider 1D manifolds in dimensions  $d = 2$ , and run all methods with their respective smallest value  $m$  required for convergence. For the proposed methods, Theorem 1.1 asks for  $m \geq 4$ ; the projection method in [15], which is identical with  $AKM_1$ , also calls for  $m \geq 4$ . KEM requires  $\tau \geq 4$  for a convergence rate of  $\tau - 3.5$  in  $\mathcal{H}^2(\mathcal{M})$ .

In Figure 1, we show the  $\mathcal{H}^2(\mathcal{M})$  and  $L^2(\mathcal{M})$  error profiles of the three methods when solving a modified Helmholtz equation in [8, Exmp.2] on the unit circle. The exact solution  $u^* = y$  was chosen so that the right side of (3.13) with  $I_Z u^*$  is small. Hence, Lemma 3.3 requires smaller  $h_X$  to hold. Both KPMs and AKMs outperform KEM in terms of accuracy and convergence rate. However, all tested methods converge faster than their respective theoretical estimates. It is also interesting to see that AKMs are slightly more accurate than KPMs; based on our numerical experiments, this occurs when  $\mathcal{M}$  is a conic section with small eccentricity.

Next, we compare our AKMs and KPMs with a Galerkin approach by means of localized spherical bases [37]. In terms of  $L^2(\mathcal{M})$  error, our method can achieve accuracy of around  $10^{-11}$  by only using 822 center points (see Figure 5.1(b)), but the less computationally intense Galerkin one obtains at most  $10^{-8}$  with  $n_Z = 961$  listed in Table 1 of the literature.

In terms of numerical costs in the case of codimension  $r = 1$ , KEM actually makes use of two extra extended copies of  $Z$  to fill up the embedding domain, i.e.,

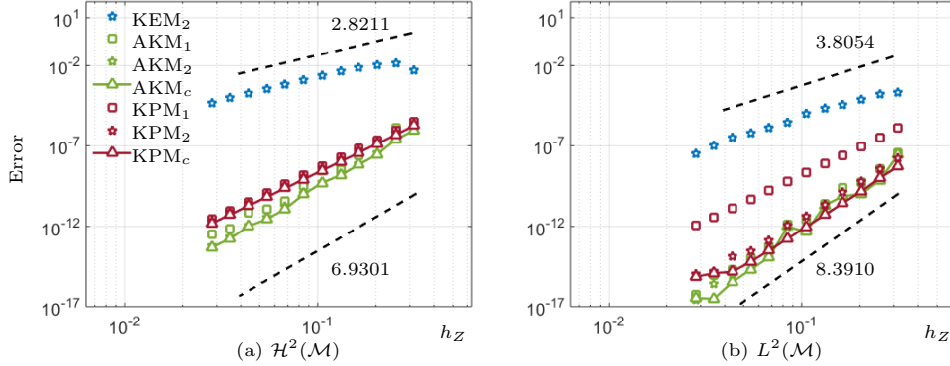


FIG. 1. The  $\mathcal{H}^2(\mathcal{M})$  and  $L^2(\mathcal{M})$  error profiles obtained by our proposed KPM and AKM methods, using  $\mathbb{R}^2$  restricted Whittle-Matérn-Sobolev kernels of smoothness order  $m = 4$ , and a kernel-based embedding (KEM) method (with  $\tau = 4$ ) for solving a modified Helmholtz equation on the unit circle. Subscripts 1, 2, and c indicate various oversampling with  $X = Z$ ,  $n_X \approx 2n_Z$ , and  $n_X \approx n_Z^3$  respectively.

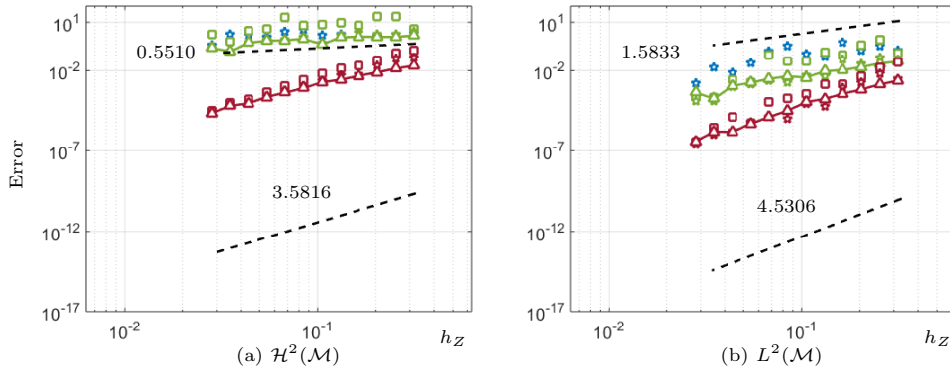


FIG. 2. The corresponding results on an ellipse with  $l_x/l_y = 5$  under the same settings as in Figure 1.

trial centers are  $\{Z, Z \pm \delta \vec{n}\}$  for some small  $\delta > 0$ . More copies are required in higher codimensions. For fair comparisons, we consider the same settings of points in  $X$  and  $Z$  on  $\mathcal{M}$  for all tested methods. In Table 1, we list the corresponding computational time of  $\text{KEM}_2$ ,  $\text{KPM}_2$ , and  $\text{AKM}_2$  in solving this example.  $\text{KEM}_2$  takes almost twice the time in solving the problem than our two methods do. Their difference of time cost are near the double with  $n_Z$  increasing, e.g.  $n_Z \geq 144$ , as listed in this table. In this experiment, we see that the most cost effective  $\text{KPM}_2$  method is also the most accurate among all.

We next perform the same test on an ellipse with the semi-major to minor ratio of  $l_x : l_y = 5 : 1$ . It was shown in [8] that, if data points are *non-uniform*, the projection method in [15] may yield highly oscillatory numerical solutions on this ellipse. In Figure 2, we show the corresponding error profiles with both  $X$  and  $Z$  being regular on the ellipse. We note that changing the geometry of  $\mathcal{M}$  results in big drops in accuracy. The estimated  $\mathcal{H}^2(\mathcal{M})$ -convergence rate of KPM drops from

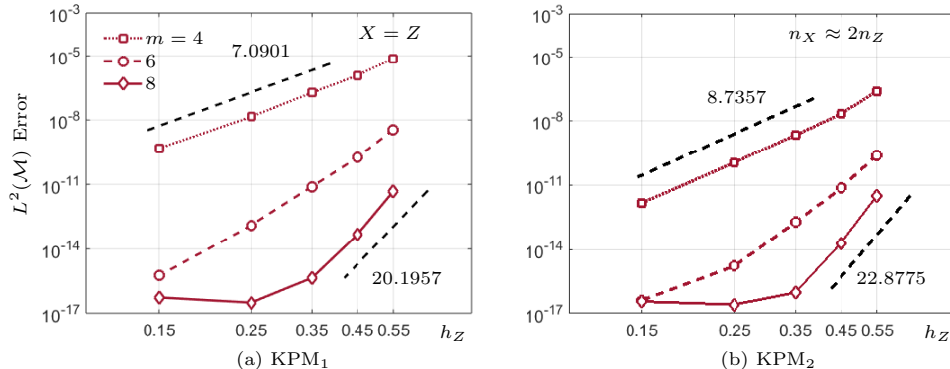


FIG. 3. The  $L^2(\mathcal{M})$  error profiles of KPMs, with and without oversampling, when solving a modified Helmholtz equation on the unit sphere with kernel of smoothness order  $m = 4, 6$  and  $8$ .

6.9 to 3.6, both of which are still higher than the 1.5 rate suggested by Theorem 1.1. The convergence rate of KEM drops from 2.8 on the unit circle to around 0.55 on this ellipse, which indeed is quite near the theoretical predicted rate of 0.5. All AKMs show similar  $\mathcal{H}^2(\mathcal{M})$  convergence, but AKMs with oversampling (i.e., AKM<sub>2</sub> and AKM<sub>c</sub>) yield more accurate solutions than KEM in terms of  $L^2(\mathcal{M})$  errors.

**5.2. Smoothness of kernels.** In this example, we further verify the convergence behaviour of the proposed methods when solving PDEs on  $\mathcal{M} \in \mathbb{R}^3$  with kernels of higher smoothness orders  $m = 4, 6$  and  $8$ .

The results from [15] have already shown that AKM performs well with  $X = Z$  on the unit sphere. Figure 3 shows the  $L^2(\mathcal{M})$  convergence profiles of KPMs that solves a modified Helmholtz equation with  $X = Z$  and  $n_X \approx 2n_Z$ . Although they are higher than the theoretical rates, the numerically observed convergence rates increase with the smoothness  $m$ . We observed that the tested KPMs converge faster than  $m$  in  $L^2(\mathcal{M})$ . For all tested  $m$ , utilizing oversampling improves accuracy.

To thoroughly compare KPM and AKM, we consider  $\mathcal{M}$  being a torus and a cyclide. On the torus, we use  $n_X \approx 2n_Z$  quasi-uniform collocation points. Because of the cyclide's non-antisymmetric geometry, it is difficult to maintain a constant ratio of  $n_X$  to  $n_Z$  for all tested  $h_Z$ ; the actual ratio ranges from 1.5 to 6 and a certain degree of oversampling is always imposed.

The resulting  $L^2(\mathcal{M})$  convergence profiles are given in Figures 4 and 5. First, all numerical convergence rates are higher than  $m$ , but the value of  $m$  does not affect the AKMs' convergence rates as much as it affects KPMs. When both methods are feasible, KPM should be given a higher priority due to its higher orders of convergence and accuracy. As for the selection of  $m$ , AKM with  $m = 6$  yields smaller error than that with  $m = 8$ . The error functions corresponding to  $m = 8$  and the smallest tested  $h_Z$  were also shown in Figures 6. A uniform error distribution on the torus can be seen; whereas the maximum error occurs on the cyclide, where curvature is high.

**5.3. Pattern formations and robustness.** The reaction diffusion equations (RDEs) [8, 15, 45, 48] are benchmarks for testing numerical methods for surface PDEs. Here, we employ our proposed KPM and AKM to generate Turing spot patterns by

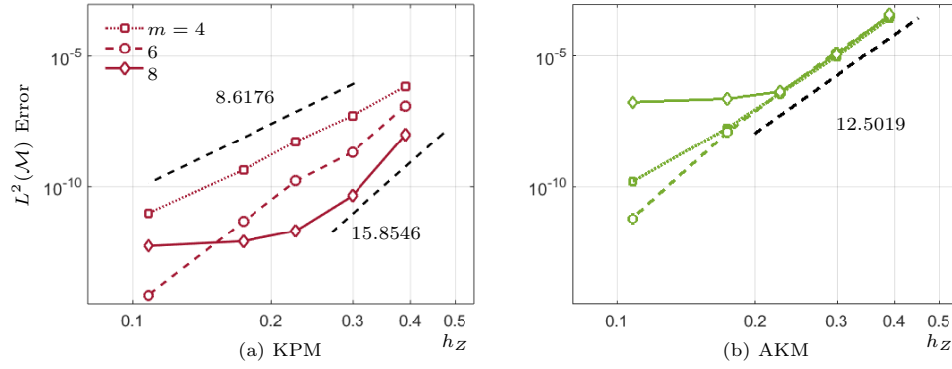


FIG. 4. The  $L^2(\mathcal{M})$  convergence profiles of the proposed KPM and AKM with kernels of different smoothness order  $m$  and with  $n_X \approx 2n_Z$  oversampling when solving a modified Helmholtz equation on a torus.

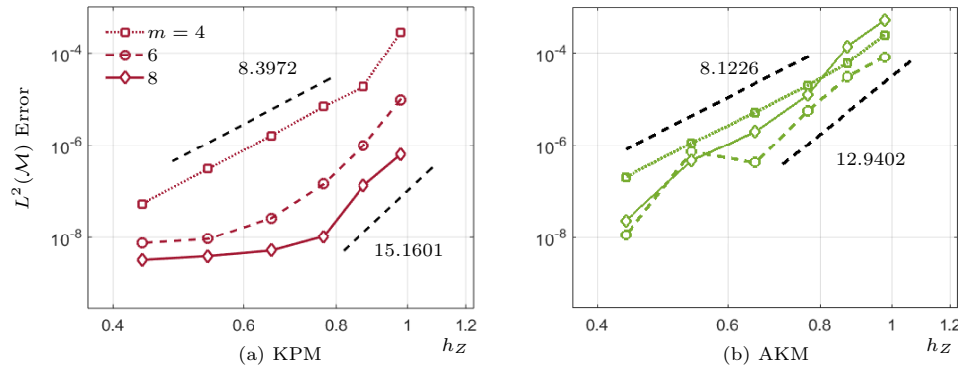


FIG. 5. The corresponding  $L^2(\mathcal{M})$  convergence results on a cyclide under the same setting as in Figure 4 and oversampling  $n_X/n_Z \in [1.5, 6]$ .

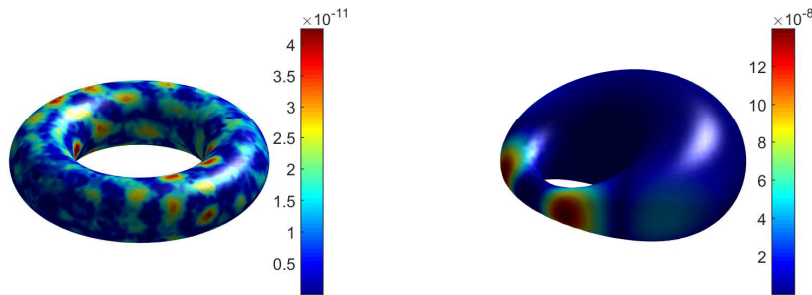


FIG. 6. The error functions of KPM with  $m = 8$  and  $h_Z = 0.11$  and  $0.44$  in Figures 4 and 5 respectively.

solving the following system of equations:

$$\begin{cases} \partial_t u = \mu \Delta_{\mathcal{M}} u + \alpha u (1 - \tau_1 v^2) + v (1 - \tau_2 u) \\ \partial_t v = \nu \Delta_{\mathcal{M}} v + \beta v \left(1 + \frac{\alpha \tau_1}{\beta} uv\right) + u (\gamma + \tau_2 v) \end{cases} \quad \text{for } x \in \mathcal{M}, t \in [0, T], \quad (5.1)$$

which models the interaction of an activator  $u$  and an inhibitor  $v$ . We use the parameters in [8] and some random initial conditions to obtain steady-state solutions on the Bretzel2 shape, see Appendix for its parametric equation. In particular, we set  $\mu = 0.516\nu$ . Smaller values of  $\nu$  yield more spots. Our aim is to study the robustness of our methods under a very economical setting in this application. We use the second-order semi-implicit backward differentiation method (SBDF2) in [3, 45] to discretize (5.1). In this approach, nonlinear terms are treated explicitly whereas the diffusion process is handled implicitly. Our proposed methods are then used to find solutions to this implicit parts in the least-squares sense.

Firstly, we consider  $\nu = \nu_1 := 8.4 \times 10^{-3}$  that gives rise to the spots on the Bretzel2 shape in Figure 7. We fixed  $m = 6$  and  $T = 500$  in this experiment. We then gradually decrease  $n_Z$ , and increase  $\Delta t$  to determine a minimal numerical setting for the KPM and AKM in generating this particular pattern. Namely, we use  $n_Z = 2082$  trial centers and a time stepping size of  $\Delta t = 0.5$ . Visually, the patterns in Figure 7 generated with  $\Delta t = 0.5$  are indistinguishable from the ones obtained with smaller  $\Delta t$ . Our economical setup is far less computational demanding than those used in [8] and comparable to those in [48]<sup>1</sup>.

To verify robustness, we run KPM and AKM with the above-found economical setup to simulate two additional higher-density spot patterns with smaller values of  $\nu_2 > \nu_3$ . Figure 8 shows that both methods successfully generate more Turing spots that are smaller in size. Continuing with  $\nu_3$ , Figure 9(a) shows that KPM can generate an even more complicated pattern with such a large  $\Delta t$ . In contrast, AKM fails to form perfectly round spots in Figure 9(b), but the algorithm does not blow up and remains stable. By refining the trial space with  $n_Z \approx 3000$  basis functions, AKM can stably produce the last pattern.

We remark that Figures 7–9 are expected to look qualitatively similar, but not quantitatively due to the use of random initial conditions. This is a property that allows similar-but-different patterns to be modeled in theoretical biology [49]. We believe the robustness of our proposed methods can help develop efficient solvers for coupled bulk-surface systems, whose applications include characterization of electro-spun membranes [41], proton diffusion along biological membranes [36], bulk mediated surface diffusion [6], and a topological insulator [16]; all of which are helpful in the development of cell biology. We leave this topic to our future study.

**6. Conclusion.** We establish a theoretical convergence analysis of a class of extrinsic kernel-based collocation methods for solving the second-order strongly elliptic PDEs on some smooth, closed, connected and complete Riemannian manifolds.

<sup>1</sup> In [8] and [48], discretization parameters used are  $(T, n_Z, \Delta t) = (400, 5000, 0.05)$  and  $(700, 12100, 0.01)$  with 31-point stencil, respectively. In this example, we used  $(500, 2082, 0.5)$  and our simulations is clearly faster than [8] due to lower computational complexity. We can compare with the finite difference approach in [48] using the above ballpark figures as follows. For any  $n_X \times n_Z$  linear system, a direct solver requires  $\mathcal{O}(n_X^2 n_Z) = \mathcal{O}(n_Z^3)$ ; the total complexity is then  $\mathcal{O}(n_Z^3 T / \Delta t)$  that is in the order of  $\sim 10^{12}$  flops. In a finite difference approach with a stencil size of  $n_s$ , solving the  $n_Z \times n_Z$  system matrix with an iterative solver would cost  $\mathcal{O}(n_s n_Z)$  per step or  $\mathcal{O}(n_s n_Z T / \Delta t)$  in total. Using a conservative guess that the iterative solver converges after 10 iterations, the cost per in the order of  $\sim 10^{11}$  flops.

We prove that the proposed methods are  $\mathcal{H}^2(\mathcal{M})$ -convergent at the rate of *at least*  $m - d_{\mathcal{M}}/2 - 2$  and numerically observed rates are usually much higher in  $\mathbb{R}^2$  and  $\mathbb{R}^3$ . Our numerical experiments also show that our proposed methods outperform a kernel-based embedded collocation method, and oversampling is beneficial to accuracy and convergence. When applied to problems of Turing pattern formations, our methods are numerically stable even with large time steps and fill distances. The meshless handling of scattered data allows easy treatment to irregular surfaces. When it comes to real-life models for cells, this is precisely what makes the proposed extrinsic methods in this paper attractive. The theoretical requirements for the methods to converge will become a useful guidebook for numerical method selection.

#### Appendix: parametric equations for all tested manifolds.

- Ellipse:  
 $\{(x, y) \in \mathbb{R}^2 | x^2/l_x^2 + y^2/l_y^2 - 1 = 0, l_x, l_y > 0\}$ .
- Cyclide:  
 $\{(x, y, z) \in \mathbb{R}^3 | (x^2 + y^2 + z^2 - 1 + 1.9^2)^2 - 4(2x + \sqrt{4 - 1.9^2})^2 - 4(1.9y)^2 = 0\}$ .
- Torus:  
 $\{(x, y, z) \in \mathbb{R}^3 | (x^2 + y^2 + z^2 + 1^2 - (1/3)^2)^2 - 4(x^2 + y^2) = 0\}$ .
- Bretzel2:  
 $\{(x, y, z) \in \mathbb{R}^3 | (x^2(1 - x^2) - y^2)^2 + 1/2z^2 - 1/40(x^2 + y^2 + z^2) = 1/40\}$ .

#### REFERENCES

- [1] R. A. ADAMS AND J. F. FOURNIER, *Sobolev spaces*, vol. 140, Academic press, 2003, [https://doi.org/10.1007/978-0-8176-4675-2\\_19](https://doi.org/10.1007/978-0-8176-4675-2_19).
- [2] R. ARCANGÉLI, M. C. L. D. SILANES, AND J. J. TORRENS, *An extension of a bound for functions in Sobolev spaces, with applications to (m, s)-spline interpolation and smoothing*, Numer. Math., 107 (2007), pp. 181–211, <https://doi.org/10.1007/s00211-007-0092-z>.
- [3] U. M. ASCHER, S. J. RUUTH, AND B. T. WETTON, *Implicit-explicit methods for time-dependent partial differential equations*, SIAM J. Numer. Anal., 32 (1995), pp. 797–823.
- [4] E. BURMAN, P. HANSBO, M. G. LARSON, A. MASSING, AND S. ZAHEDI, *Full gradient stabilized cut finite element methods for surface partial differential equations*, Comput. Methods Appl. Mech. Engrg., 310 (2016), pp. 278–296.
- [5] D. A. CALHOUN AND C. HELZEL, *A finite volume method for solving parabolic equations on logically Cartesian curved surface meshes*, SIAM J. Sci. Comput., 31 (2009), pp. 4066–4099, <https://doi.org/10.1137/08073322x>.
- [6] A. V. CHECHKIN, I. M. ZAID, M. A. LOMHOLT, I. M. SOKOLOV, AND R. METZLER, *Bulk-mediated diffusion on a planar surface: Full solution*, Phys. Rev. E, 86 (2012), p. 041101.
- [7] C. S. CHEN, C. M. FAN, AND P. H. WEN, *The method of approximate particular solutions for solving elliptic problems with variable coefficients*, Int. J. Comput. Methods, 8 (2011), pp. 545–559, <https://doi.org/10.1142/s0219876211002484>.
- [8] K. C. CHEUNG AND L. LING, *A kernel-based embedding method and convergence analysis for surfaces PDEs*, SIAM J. Sci. Comput., 40 (2018), pp. A266–A287.
- [9] K. C. CHEUNG, L. LING, AND R. SCHABACK, *H<sup>2</sup>-convergence of least-squares kernel collocation methods*, SIAM J. Numer. Anal., 56 (2018), pp. 614–633.
- [10] G. DZIUK, *Finite elements for the Beltrami operator on arbitrary surfaces*, Springer Berlin Heidelberg, 1988, <https://doi.org/10.1007/bfb0082865>.
- [11] E. FUSELIER, T. HANGELBROEK, F. J. NARCOWICH, J. D. WARD, AND G. B. WRIGHT, *Localized bases for kernel spaces on the unit sphere*, SIAM J. Numer. Anal., 51 (2013), pp. 2538–2562.
- [12] E. FUSELIER, F. NARCOWICH, J. WARD, AND G. WRIGHT, *Error and stability estimates for surface-divergence free RBF interpolants on the sphere*, Math. Comp., 78 (2009), pp. 2157–2186.
- [13] E. FUSELIER AND G. B. WRIGHT, *Scattered data interpolant on embedded submanifolds with restricted positive definite kernels: Sobolev error estimates*, SIAM J. Numer. Anal., 50 (2012), pp. 1753–1776, <https://doi.org/10.1137/110821846>.
- [14] E. J. FUSELIER AND G. B. WRIGHT, *Stability and error estimates for vector field interpolation and decomposition on the sphere with RBFs*, SIAM J. Numer. Anal., 47 (2009), pp. 3213–

- 3239.
- [15] E. J. FUSELIER AND G. B. WRIGHT, *A high-order kernel method for diffusion and reaction-diffusion equations on surfaces*, J. Sci. Comput., 56 (2013), pp. 535–565, <https://doi.org/10.1007/s10915-013-9688-x>.
  - [16] I. GARATE AND L. GLAZMAN, *Weak localization and antilocalization in topological insulator thin films with coherent bulk-surface coupling*, Phys. Rev. B, 86 (2012), p. 035422.
  - [17] P. GIESL AND H. WENDLAND, *Meshless collocation: Error estimates with application to dynamical systems*, SIAM J. Numer. Anal., 45 (2007), pp. 1723–1741, <https://doi.org/10.1137/060658813>.
  - [18] J. B. GREER, *An improvement of a recent Eulerian method for solving PDEs on general geometries*, J. Sci. Comput., 29 (2006), pp. 321–352, <https://doi.org/10.1007/s10915-005-9012-5>.
  - [19] N. GROSSE AND C. SCHNEIDER, *Sobolev spaces on Riemannian manifolds with bounded geometry: General coordinates and traces*, Math. Nachr., 286 (2013), pp. 1586–1613, <https://doi.org/10.1002/mana.201300007>.
  - [20] T. HANGELBROEK, F. J. NARCOWICH, C. RIEGER, AND J. D. WARD, *Direct and inverse results on bounded domains for meshless methods via localized bases on manifolds*, in Contemporary Computational Mathematics - A Celebration of the 80th Birthday of Ian Sloan, J. Dick, F. Kuo, and H. Wozniakowski, eds., Springer, 2018, pp. 517–543.
  - [21] F. HAUSSEY AND A. VOIGT, *A discrete scheme for parametric anisotropic surface diffusion*, J. Sci. Comput., 30 (2007), pp. 223–235, <https://doi.org/10.1007/s10915-005-9064-6>.
  - [22] Y. C. HON AND R. SCHABACK, *On unsymmetric collocation by radial basis functions*, Appl. Math. Comput., 119 (2001), pp. 177–186, [https://doi.org/10.1016/s0096-3003\(99\)00255-6](https://doi.org/10.1016/s0096-3003(99)00255-6).
  - [23] E. J. KANSA, *Multiquadrics-A scattered data approximation scheme with applications to computational fluid-dynamics-I surface approximations and partial derivative estimates*, Comput. Math. Appl., 19 (1990), pp. 127–145, [https://doi.org/10.1016/0898-1221\(90\)90270-t](https://doi.org/10.1016/0898-1221(90)90270-t).
  - [24] E. J. KANSA, *Multiquadrics-A scattered data approximation scheme with applications to computational fluid-dynamics-II solutions to parabolic, hyperbolic and elliptic partial differential equations*, Comput. Math. Appl., 19 (1990), pp. 147–161, [https://doi.org/10.1016/0898-1221\(90\)90271-k](https://doi.org/10.1016/0898-1221(90)90271-k).
  - [25] E. J. KANSA AND G. JUERGEN, *Numerical solution to time-dependent 4D inviscid Burgers' equations*, Eng. Anal. Boundary Elem., 37 (2013), pp. 637–645, <https://doi.org/10.1016/j.enganabound.2013.01.003>.
  - [26] Q. T. LE GIA, I. H. SLOAN, AND H. WENDLAND, *Multiscale analysis in Sobolev spaces on the sphere*, SIAM J. Numer. Anal., 48 (2010), pp. 2065–2090.
  - [27] Q. T. LE GIA, I. H. SLOAN, AND H. WENDLAND, *Multiscale RBF collocation for solving PDEs on spheres*, Numer. Math., 121 (2012), pp. 99–125.
  - [28] W. LI, M. LI, C. S. CHEN, AND X. LIU, *Compactly supported radial basis functions for solving certain high order partial differential equations in 3D*, Eng. Anal. Boundary Elem., 55 (2015), pp. 2–9, <https://doi.org/10.1016/j.enganabound.2014.11.012>.
  - [29] L. LING, R. OPFER, AND R. SCHABACK, *Results on meshless collocation techniques*, Eng. Anal. Boundary Elem., 30 (2006), pp. 247–253, <https://doi.org/10.1016/j.enganabound.2005.08.008>.
  - [30] L. LING AND R. SCHABACK, *Stable and convergent unsymmetric meshless collocation methods*, SIAM J. Numer. Anal., 46 (2008), pp. 1097–1115, <https://doi.org/10.1137/06067300x>.
  - [31] C. B. MACDONALD AND S. J. RUUTH, *Level set equations on surfaces via the closest point method*, J. Sci. Comput., 35 (2008), pp. 219–240, <https://doi.org/10.1007/s10915-008-9196-6>.
  - [32] C. B. MACDONALD AND S. J. RUUTH, *The implicit closest point method for the numerical solution of partial differential equations on surfaces*, SIAM J. Sci. Comput., 31 (2009), pp. 4330–4350, <https://doi.org/10.1137/080740003>.
  - [33] T. MÄRZ AND C. B. MACDONALD, *Calculus on surfaces with general closest point functions*, SIAM J. Numer. Anal., 50 (2012), pp. 145–189, <https://doi.org/10.1137/120865537>.
  - [34] T. MÄRZ, P. ROCKSTROH, AND S. J. RUUTH, *An embedding technique for the solution of reaction-diffusion equations on algebraic surfaces with isolated singularities*, J. Math. Anal. Appl., 436 (2016), pp. 911–943, <https://doi.org/10.1016/j.jmaa.2015.11.064>.
  - [35] B. MATÉRN, *Spatial variation*, vol. 36, Springer Science & Business Media, 2013.
  - [36] E. MEDVEDEV AND A. STUCHEBRUKHOV, *Proton diffusion along biological membranes*, J Phys Condens Matter, 23 (2011), p. 234103.
  - [37] F. J. NARCOWICH, S. T. ROWE, AND J. D. WARD, *A novel Galerkin method for solving PDEs on the sphere using highly localized kernel bases*, Math. Comput., 86 (2017), pp. 197–231,

- <https://doi.org/10.1090/mcom/3097>.
- [38] F. J. NARCOWICH, X. SUN, AND J. D. WARD, *Approximation power of RBFs and their associated SBFs: A connection*, Adv. Comput. Math., 27 (2007), pp. 107–124, <https://doi.org/10.1007/s10444-005-7506-1>.
  - [39] F. J. NARCOWICH, J. D. WARD, AND G. B. WRIGHT, *Divergence-free RBFs on surfaces*, J. Fourier Anal. Appl., 13 (2007), pp. 643–663.
  - [40] J. NASH, *The imbedding problem for Riemannian manifolds*, Ann. Math., (1956), pp. 20–63.
  - [41] D. R. NISBET, A. E. RODDA, D. I. FINKELSTEIN, M. K. HORNE, J. S. FORSYTHE, AND W. SHEN, *Surface and bulk characterisation of electrospun membranes: Problems and improvements*, Colloids Surf., B, 71 (2009), pp. 1–12.
  - [42] G. PANG, W. CHEN, AND Z. FU, *Space-fractional advection-dispersion equations by the Kansa method*, J. Comput. Phys., 293 (2015), pp. 280–296, <https://doi.org/10.1016/j.jcp.2014.07.020>.
  - [43] P.-O. PERSSON AND G. STRANG, *A simple mesh generator in MATLAB*, SIAM Rev., 46 (2004), pp. 329–345, <https://doi.org/10.1137/S0036144503429121>.
  - [44] C. PIRET, *The orthogonal gradients method: A radial basis functions method for solving partial differential equations on arbitrary surfaces*, J. Comput. Phys., 231 (2012), pp. 4662–4675, <https://doi.org/10.1016/j.jcp.2012.03.007>.
  - [45] S. J. RUUTH, *Implicit-explicit methods for reaction-diffusion problems in pattern formation*, J. Math. Biol., 34 (1995), pp. 148–176, <https://doi.org/10.1007/bf00178771>.
  - [46] S. J. RUUTH AND B. MERRIMAN, *A simple embedding method for solving partial differential equations on surfaces*, J. Comput. Phys., 227 (2008), pp. 1943–1961, <https://doi.org/10.1016/j.jcp.2007.10.009>.
  - [47] R. SCHABACK, *All well-posed problems have uniformly stable and convergent discretizations*, Eng. Anal. Boundary Elem., 132 (2016), pp. 597–630, <https://doi.org/10.1007/s00211-015-0731-8>.
  - [48] V. SHANKAR, G. B. WRIGHT, R. M. KIRBY, AND A. L. FOGELSON, *A radial basis function (RBF)-finite difference (FD) method for diffusion and reaction-diffusion equations on surfaces*, J. Sci. Comput., 63 (2015), pp. 745–768, <https://doi.org/10.1007/s10915-014-9914-1>.
  - [49] A. M. TURING, *The chemical basis of morphogenesis*, Philos. Trans. Royal Soc. B: Biological Sciences, 237 (1952), pp. 37–72.
  - [50] K. UMEZU,  *$L^p$  approach to mixed boundary value problems for second-order elliptic operators*, Tokyo J. of Math., 17 (1994), pp. 101–123, <https://doi.org/10.3836/tjm/1270128189>.
  - [51] H. WENDLAND, *Error estimates for interpolation by compactly supported radial basis functions of minimal degree*, J. Approx. Theory, 93 (1998), pp. 258–272, <https://doi.org/10.1006/jath.1997.3137>.
  - [52] H. WENDLAND, *Scattered data approximation*, vol. 17, Cambridge university press, 2004.
  - [53] H. WENDLAND, *A high-order approximation method for semilinear parabolic equations on spheres*, Mathematics of Computation, 82 (2013), pp. 227–245.
  - [54] J. WLOKA, *Partial Differential Equations*, Cambridge University Press, 1987, <https://doi.org/10.1017/cbo9781139171755>.

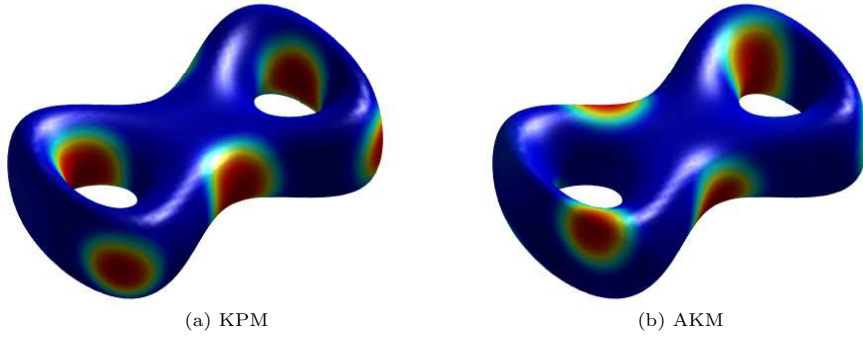


FIG. 7. Model patterns associated with  $\nu_1$  for identifying a large  $\Delta t = 0.5$  that allows the KPM and AKM to complete the Turing spot formations successfully.

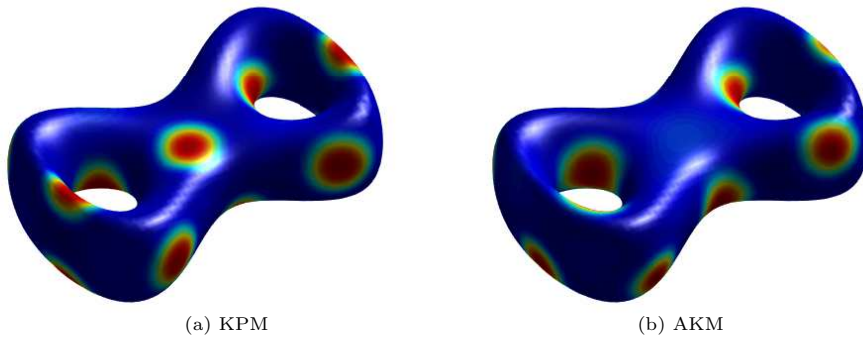


FIG. 8. The KPM and AKM simulated results with  $\nu_2 (< \nu_1)$  under the same economical setting as in Figure 7.

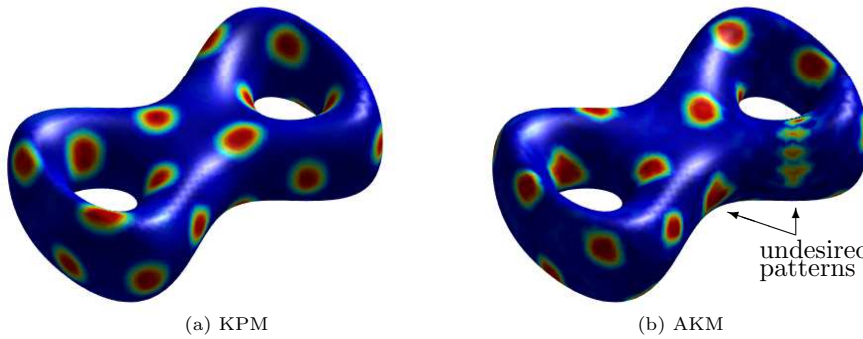


FIG. 9. The KPM and AKM simulated results with  $\nu_3 (< \nu_2 < \nu_1)$  under the same economical setting as in Figure 7.